Nuclear Theory'22
ed. V. Nikolaev, Heron Press, Sofia, 2003

# Microscopic Cranking Approach of Nuclear Rotational Modes Including Pairing Correlations with Particle Number Conservation

**J. Libert**[1], **H. Laftchiev**[2], **and P. Quentin**[3]

[1]IPN-Orsay, CNRS-IN2P3 Université Paris XI,
15 rue Georges Clémenceau F-91406 Orsay France

[2]Institute of Nuclear Research and Nuclear Energy,
Bulgarian Academy of Sciences, Sofia 1784, Bulgaria

[3]CENBG CNRS IN2P3-Université Bordeaux I,
F-33175 Gradignan cedex France

**Abstract.**

An approximation dubbed as the Higher Tamm–Dankoff Approximation (HTDA) has been designed to treat microscopically pairing correlations within a particle number conserving approach. It relies upon a n particle - n hole expansion of the nuclear wave-function. It is applied here for the first time in a rotating frame, i.e. a self-consistent cranking approach (Cr.HTDA) devoted to the description of collective rotational motion in well-deformed nuclei. Moments of inertia predicted by Cr.HTDA in the yrast superdeformed (SD) bands of $^{192}$Hg and $^{194}$Pb are compared with values deduced from experimental SD sequences and with those produced by the current Cranking Hartree–Fock–Bogoliubov approach under similar hypotheses.

## 1 Introduction

The study of nuclear structure has met during the past few years many and impressives successes using effective phenomenological nucleon-nucleon forces. On this microscopic ground, various descriptions of nuclear phenomena became precise enough to reach a predictive character, and to demonstrate convincingly their ability to model the nuclear behavior. This includes rotational collective

modes, especially theoretical and experimental studies of superdeformed (SD) bands, on which a lot of efforts. has been focused. As well known these sequences provide a stringent test for dynamical approaches in which rotational modes are decoupled from other degrees of freedom . The most developed quasiparticle variational approaches - the HFB (Hartree-Fock-Bogoliubov) and the RHB (Relativistic Hartree-Bogoliubov) approximations, combined with approximate projection methods (to restore the broken symmetries of particle number, angular momentum etc...) are the state of the art in the study of rotational bands in heavy nuclei. They were used in many calculations to reproduce quantitatively the inertial properties of the SD bands, in particular in the $A \sim 190$ region. In this region where the SD phenomenon is observed from very low spin to very high spins, the behavior of the moment of inertia as a function of the angular momentum is directly connected with the evolution of the pairing field. Therefore any microscopic approach able to reproduce this function relies upon three essential points:

1. A theory giving a reasonable value of the moment of inertia at low spin. Following Ref. [1], in which rotation and vibrations are treated on the same ground within an adiabatic approach valid at low spin, "reasonable" means in the present context 10-15% higher than the experimental value. Within our microscopical contexts, success on that aspect is mainly governed by the pairing strengths values. As seen hereafter, our present objective is not to discuss pairing strengths but to compare the behavior of moment of inertia deduced from different approaches of rotation. We will therefore adjust their respective pairing strengths to start the rotational sequence in a reasonable agreement between themselves and with experimental data. As it will be shown, the adopted pairing strengths will lead us at low spin with wave-functions having the same "amount of correlations" (under the definition of a consistent measure for that).

2. A deep understanding of the so-called Coriolis Anti-Pairing mechanism which governs the decrease of pairing correlation with angular momentum. As a common result of microscopical theories for the $^{192}$Hg and $^{194}$Pb, yrast SD bands on which the present study is centered, it should be noticed that the behavior of the corresponding moments of inertia cannot not be connected with a change in deformation on increasing spin. It is rather due with a change of intrinsic properties i.e. the balance between normal and superfluid currents [2].

3. A theory remaining valid in the low pairing context which should anyway appear at medium or high spin in a SD band of the $A \sim 190$ region. In that respect, the BCS or Bogoliubov quasiparticle approximations are known to be faulty, giving rise to spurious normal superfluid transitions when the gap between the last occupied and the first unoccupied single

particle level increases. Of course such transitions have tremendous effects on collective kinetic energies and therefore on the deduced tensor of inertia. This third point constitues clearly the basic motivation to develop a Higher Tamm Dancoff Approaches (HTDA) in which pairing corrrelations are present, but where the quasiparticle approximation is avoided together with its most undesirable effects as the spreading in number of particle and, as it will be shown, these spurious transitions.

The Hg–Pb yrast SD bands served as a testing place for many theoretical microscopic approaches. In the famework of the Cranked HFB (Cr. HFB) approach, calculations in this region have been initiated with Skyrme force on the particle-hole channel and seniority or $\delta$ forces in the particle particle one [3]. Similar approaches have been developped simultaneously with the D1S Gogny force [4]. As understood long time ago, the Gaussian form (i.e. those of the Gogny force) gives a more robust behavior of the pairing field on increasing the Fermi gap. As a consequence, drastic accidents in the moment of inertia have been historically considered first in calculation using seniority or $\delta$ pairing forces. Various attemps to cure them have been rapidly implemented in this context, in particular the Lipkin-Nogami (LN) approximate restoration of the number of particles which produces more correlated solutions and therefore (see Ref. [5]) delays the problem to higher spin. LN or similar approximate projections techniques have been finally also implemented in Cr.HFB calculations with Gogny forces [6], [7]. Finally, the LN solutions show in this case the worst behavior of the inertial moments against the non-projected ones when comparing with the experiment, as shown in Ref. [7]. That corresponds to a severe limitation of this approximate projection technique when the low-pairing regime is reached (see Fig. 10.9 in Ref. [7]).

Some HFB+LN calculations with the Skyrme force on the particle-hole channel and surface-activated zero-range delta pairing interaction were done for $^{192}$Hg in Ref. [8]. Similarily to the results obtained with the Gogny force, the trends of their inertial moments reproduce the data relatively well qualitatively, but not at all in quantitatively correct way. The same is true also for the RHB calculations discussed in Ref. [9]. For instance, for all these calculations, when using a Lipkin-Nogami approximate projection technique, it is found that the $J^{(2)}$ moment of inertia deviates too much from data when the angular velocity $\omega$ become greater than 0.3 MeV/$\hbar$ (i.e. in a low pairing region). Thus, being a testing place for many approaches, the first SD band of $^{192}$Hg still waits for a correct theoretical description.

The HTDA approximation was proposed to allow the theoretical modelling of heavy nuclei taking into account pairing correlations without breaking the particle number symmetry (see for instance Refs. [10] and [11]). Being in spirit very close to the traditional shell model approaches, it gives solutions as eigenstates of the number of particles and eliminates the problem. Applying this approach

to the yrast SD band of $^{192}$Hg and $^{194}$Pb nuclei, we present here the very first test of the cranked version of this approach (Cr. HTDA). The article is structured as follows. In Section 2, we describe briefly the Cr. HTDA approach, the pairing interaction and the symmetries properties of our cranked hamiltonian. In Section 3, we present and discuss the results of the Cr. HTDA calculations for yrast SD bands of $^{192}$Hg and $^{194}$Pb, comparing them together with experimental data and with the corresponding Cr. HFB results using similar forces. Section 4 is finally devoted to a summary of our results, together with conclusions and perspectives offered by this new approach.

## 2 The Cranked HTDA Approach

### 2.1 The Grounds for HTDA

The static HTDA method has been described in Refs. [10] and [11]. Let us recall the three main steps upon which it relies:

i) A $n$ particule -$n$ hole Slater determinant basis set is built on a "vacuum" Hartree-Fock solution associated with the one-body density matrix $\rho^0$ and the corresponding selfconsistent HF hamiltonian $h^0\left(\rho^0\right)$. In the present work, this mean field is built on the ground of the Skyrme SKM$^*$ parametrization of the effective nucleon-nucleon interaction.

ii) Introducing a $\delta$ pairing interactiong and deducing its contributions of the "mean field" type leads us to the residual interaction $V_0^{res}$ and therefore to the hamiltonian $H_0^{HTDA} = h^0(\rho^0) + V_0^{res}$. The corresponding Schrödinger equation is solved. In practice, only the state with the lowest energy is of present physical interest, (namely $\Psi$). It is extracted using standard Lanczös algorithm and formally writes :

$$|\Psi\rangle = |\phi_0\rangle + \sum_{i=\forall\, 1p1h} \chi_1^i \left|\phi_1^i\right\rangle + \sum_{j=\forall\, 2p2h} \chi_2^j \left|\phi_2^j\right\rangle + \sum_{k=\forall\, 3p3h} \chi_3^k \left|\phi_3^k\right\rangle + \ldots , \quad (1)$$

where the many-body ground-state wave-function is described by the Slater determinant $|\phi_0\rangle$ built with the N or Z lowest energy sp states. When promoting a nucleon from a hole state $\varphi_a$ to a particle state $\varphi'_a$ neglecting the mean-filed changes, one gets a new determinant $\left|\phi_1^i\right\rangle$ which corresponds to the particular 1 particle -1 hole excitation (1p1h) associated with the exchange of $\varphi_a$ by $\varphi'_a$. In this way, one built the many-body basis of Slater determinants $\left|\phi_2^j\right\rangle$, $\left|\phi_3^k\right\rangle$ ..., corresponding to 2 particles -2 holes (2p2h), 3 particles -3 holes (3p3h) ... excitations of the reference quasivacuum Slater determinant $|\phi_0\rangle$. Within this space, the N-(or

Z) body wave-function is finally represented by the expansion coefficients $\chi_n^m$. The basis of Slater determinant $|\phi_n^m\rangle$ is of course infinite and has to be truncated to be handled by computers. That point will be discussed hereafter.

iii) From the correlated wave-function $\Psi_{\alpha=0}$written as the combination of Slater determinants Eq. (1), one deduces a new one-body density:

$$(\rho_{\alpha=1}^{corr})_{ij} = \left\langle \Psi_{\alpha=0} \left| a_j^+ a_i \right| \Psi_{\alpha=0} \right\rangle \tag{2}$$

which defines through Skyrme functional a new one body Hamiltonian $h^0(\rho_{\alpha=1}^{corr})$, whose solutions define a new set of n particule -n hole states (step i). The HTDA Hamiltonian writes in this new space $H_{\alpha=1}^{HTDA} = h^0(\rho_{\alpha=1}^{corr}) + V_{\alpha=1}^{res}$ from which the new correlated wave-function (step ii) is extracted as $\Psi_{\alpha=1}$, the process being pursued increasing the index $\alpha$ up to convergence.

## 2.2 The Cranked HTDA Hamiltonian

These basic principles have been kept in the present routhian approach, in which a linear constraint on the component $J_x$ of the angular momentum is added, writing therefore the "Hamiltonian":

$$\widehat{H} = \widehat{H}_{Skyrme} + \widehat{H}_{Coulomb} + \widehat{H}_{pair} - \omega \widehat{J}_x \tag{3}$$

where $\widehat{H}_{pair}$ is nothing but the residual interaction $V^{res}$ deduced for a given space from the $\delta$ pairing interaction, and where $\omega$ is the angular velocity i.e. the Lagrange multiplier associated with the dynamical constraint $\widehat{J}_x$.

Eq. (1) is used to write the HTDA Hamiltonian matrix of in the $npnh$ representation:

$$H_{ij} = \left\langle \phi_n^i | \widehat{H} | \phi_m^j \right\rangle = \begin{array}{c} \\ \text{0p0h} \\ \text{1p1h} \\ \text{2p2h} \\ \text{...} \end{array} \begin{array}{c} \begin{array}{cccc} \text{0p0h} & \text{1p1h} & \text{2p2h} & \text{...} \end{array} \\ \begin{pmatrix} H_{00} & H_{01} & H_{02} & \text{...} \\ H_{10} & H_{11} & H_{12} & \text{...} \\ H_{20} & H_{21} & H_{22} & \text{...} \\ \text{...} & \text{...} & \text{...} & \text{...} \end{pmatrix} \end{array} \tag{4}$$

One neglects the changes of the mean field caused by the $npnh$ excitations. Thus, mean field contributions vanish in the non diagonal terms of (4):

$$\left\langle \phi_n^i | \widehat{H}_{Skyrme} + \widehat{H}_{Coulomb} - \omega \widehat{J}_x | \phi_m^j \right\rangle = H_{00} + \delta_{ij} (\sum_p e_p^i - \sum_h e_h^i) \tag{5}$$

Here $e_h$ and $e_p$ are the energies of the hole and particle excitation states in $\phi_n^i$ with respect to $\phi_0$, $H_{00} = \langle \phi_0 | K + V_{HF} | \phi_0 \rangle$ is the total energy of the quasivacuum Slater determinant. The non-diagonal matrix elements are only due to the

residual interaction defined as:

$$\widehat{V}^{res} = \widehat{V} - \widehat{V}_{HF} \ , \tag{6}$$

where $\widehat{V}$ is the two-body interaction including all interactions and $\widehat{V}_{HF}$ is the one-body reduction of the Skyrme and Coulomb interactions. The non-diagonal matrix elements of $\widehat{H}$ are thus given by:

$$H_{ij} = \left\langle \phi_n^i | \widehat{V}^{res} | \phi_m^j \right\rangle \ . \tag{7}$$

It is computed with the help of the Wick's theorem as detailed in Refs. [10] and [11].

### 2.3 The Zero-Range Pairing Force

Due to a well known divergence of the theory, we limit the action of our residual interaction (we use a volume zero-range pairing one - see Ref. [12] – similar to that employed in static HTDA calculation of Refs. [10] and [11]) to states whose energies are in the vicinity of the Fermi energy $\lambda$. To avoid any artificial sharp cutoff energy dependance (due to the appearance or disappearance of some single particle state into the window upon varying any continuous parameter like $\omega$), it is customary to introduce a smoothing factor $f(e_i)$ defined by a cutoff parameter $X$ (in present case $X = 4$ MeV) and a smoothing parameter $\mu$ (here, $\mu = 0.2$ MeV) and written as:

$$f^2(e_i) = \frac{\left(1 + exp\left(-\dfrac{X}{\mu}\right)\right)}{\left(1 + exp\left(\dfrac{(e_i - \lambda) - X}{\mu}\right)\right)} \ . \tag{8}$$

The matrix element of the interaction takes then the form :

$$\widetilde{V}_{ijkl}^{pair} = V_0 \left\langle ij \left| \frac{1 - \overrightarrow{\sigma}_1 . \overrightarrow{\sigma}_2}{4} \, \delta(\overrightarrow{r}_1 - \overrightarrow{r}_2) \right| \widetilde{kl} \right\rangle \, f(e_i) \, f(e_j) \, f(e_k) \, f(e_l) \ , \tag{9}$$

where $V_0$ is the pairing strength for a given isospin, and where $\sigma_i$ are the usual Pauli matrices. Finally, $V_0$ values will be discussed and produced hereafter in section 3.1.

### 2.4 The Cut-Off in the Many-Body Basis

In such a shell-model like problem, the corner stone is clearly to determine the size of the $npnh$ basis which will give a convincing accuracy and convergence of solution states. Four main remarks will allow us to keep with Cr. HTDA a numerically tractable problem:

1. As it is extensively employed in shell model calculations, it is worth noting that a large amount of coefficients in the expansion Eq. (1) are known a priori to have zero value. That allows to introduce various numerical recipes to deal with non-zero terms only. Prescriptions eliminating the stockage of very weak matrix elements are also employed to minimize calculation time and storage.

2. As shown previously, the HTDA reference quasivacuum is built iteratively in such a way that it contains the changes in the mean filed due to correlations. That is done using the correlated sp density matrix Eq. (2) to derive the Skyrme one body hamiltonian giving the HTDA reference quasivacuum. That defines an optimal way to get the quasivacuum. Therefore, the HTDA approach which is a highly truncated kind of shell model, exhibits some kind of bigger generality in its nature: The self-consistent procedure is contributing to a more general level-mixing, taking into account the mean field changes due to the correlated density matrix. The optimized character of the HTDA reference quasivacuum state has been shown clearly in static calculations of Refs. [10] and [11].

3. To reduce the basis size, the present HTDA approach takes clearly advantage of the particular form of the interaction. The cutoff parameter Eq. (8) involved in the pairing interaction matrix elements Eq. (9) introduces de facto a cutoff in the list of the Slater determinants to be taken into account in the space: As matter of fact, the matrix elements $H_{ij}$ $(i \neq j)$ are zero for all determinants $\phi_n^i$, $\phi_m^j$ which include excitation hole and particle sp states beyond the allowed interval (here it is $[\lambda - X - (5/2)\mu, \lambda + X + (5/2)\mu]$). Therefore, this property of the residual interaction limits the excitation energies of the $\phi_1$ determinants to 2X+5$\mu$. Coherently with the truncation for the 1p1h excitations, we limit also to this value the excitation energies of the 2p2h excitations etc...

4. The HTDA calculations for the ground state and the K-isomer states of $^{178}$Hf of Refs. [10] and [11] have shown moreover that, in similar conditions, the properties of the $\delta$ pairing interaction are such that the inclusion of 3p3h and 4p4h excitation states does not significantly changes the total energy of the solution. In present work, we have therefore restricted ourselves to the (0p0h,1p1h,2p2h) part of the space.

As a conclusion of the present subsection one will retain that the basis of Slater determinants is truncated mostly due to the properties of the zero-range delta pairing interaction. That gives in practice, in each symmetry blocks discussed hereafter a typical basis size around 10 000, remaining therefore in the range of tractable nuclear microscopic approaches. As already said, to extract a few eigenstates and eigenvalues in such blocks, it is efficient to use the the

Lanczos algorithm. Practically, in this purpose, we have employed the numerical code written by B. N. Parlett and D. S. Scott [13] available as an open source.

### 2.5 Symmetries of the Cr. HTDA Hamiltonian

It is shown for instance in Ref. [5] and in Ref. [14] (See also Ref. [15]) that the HF (and also the HFB) cranking Skyrme Hamiltonian preserves the symmetries in parity and signature. The corresponding sp spectrum (and the n particles – n holes deduced Slater determinants) are also parity-signature symmetric. The selection rules for the zero-range volume pairing interaction when using sp states with good parity-signature symmetries are:

$$V_{ijkl}^{pair} = 0, \quad \text{when} \;\; s_i s_j s_k s_l \neq 1 \;\; \text{or} \;\; \pi_i \pi_j \pi_k \pi_l \neq 1 \; ,$$

where $s_i$, $s_j$, $s_k$, $s_l$ and $\pi_i$, $\pi_j$, $\pi_k$, $\pi_l$ are signatures and parities of the sp states with indexes $i$, $j$, $k$, and $l$ respectively. When taking these rules into account, it is straightforward to verify through the Wick's theorem from Eqs. (7 and 9) that the Hamiltonian matrix become block-diagonal regarding the four types of Slater determinants in the basis: those which have the same parity and signature as the quasivacuum $|\phi_0\rangle$ has, those with only the parity changed, those which change only the signature and those which have the opposite parity and signature. This allows us to diagonalize separately in four blocks for each isospin. Of course, the final result is in the block which gives the lowest total energy $\left\langle \widehat{H} \right\rangle = \left\langle \Psi | \widehat{H} | \Psi \right\rangle$. It defines a ground state $\Psi$ for which the expansion Eq. (1) is made over Slater determinants having all the same properties in parity and signature (and isospin). The deduced one-body $\rho^{corr}$ density matrix Eq. (2), is block-diagonal toward the same parity-signature symmetry and hence the diagonalization of the symmetric functional $H_{HF}(\rho_{ij}^{corr})$ gives a new quasivacuum $|\phi_0\rangle$ with good parity-signature quantum numbers. The self-consistent cranking HTDA Hamiltonian generate a real decomposition for the sp and many-body states, when one has real trial functional $H_{HF}(\rho_{ij})$ at the begining. Therefore, the cranking-HTDA solution with Skyrme and zero-range volume pairing interactions is real and symmetric under the parity and signature (as defined in Ref. [14]) transformations.

The present HTDA Hamiltonian can be decomposed in two parts:

$$H_{ij} = H_{00}\delta_{ij} + \begin{pmatrix} 0 & 0 & \widehat{V}_{02}^{res} \\ 0 & \widehat{V}_{11}^{res} + e_p^i - e_h^i & \widehat{V}_{12}^{res} \\ \widehat{V}_{20}^{res} & \widehat{V}_{21}^{res} & \widehat{V}_{22}^{res} + \sum_p e_p^i - \sum_h e_h^i \end{pmatrix} = \\ = M_1 + M_2 \; , \quad (10)$$

where $\widehat{V}_{mn}^{res}$ is a short notation for $\left\langle \phi_m^i | \widehat{V}^{res} | \phi_n^j \right\rangle$. In this decomposition, the first (diagonal) part $M_1$ remain unchanged by the diagonalisation process. We

therefore diagonalise only the $M_2$ part and the resulting eigenstates are eigenstates for $M_1 + M_2$ too. The total energy is finaly $E_{tot} = H_{00} + E_{corr}$ where the correlation energy $E_{corr}$ is the eigenstate of the $M_2$ matrix and is a possible measure for the strength of the pairing correlations, eventhough it contains not only correlations of the pairing type.

### 2.6 Triaxial Deformation and Angular Momentum

Mean values of the projection of the angular momentum on the rotational axis $\widehat{J}_x = \widehat{L}_x + \widehat{S}_x$ and of the quadrupole deformation moments ($\widehat{Q}_{20}$ and $\widehat{Q}_{00}$) operators are deduced as any other single particle operators through summations involving the density matrix $\rho_{ij}^{corr}$ (Eq. (2)) of the general form:

$$\left\langle \widehat{F} \right\rangle = \sum_{ij} f_{ij} \rho_{ji}^{corr} \ . \tag{11}$$

Finally, as in any Cranking model, constraint on $\left\langle \widehat{J}_x \right\rangle$ (which is a one body term entering $H_{00}$) is related to the total angular momentum $I$ through the standard semiclassical condition associated with the hypothese of a pure rotation around the $x$-axis, condition which writes namely:

$$\left\langle \widehat{J}_x \right\rangle = \sqrt{I\ (I+1)} \tag{12}$$

which fixes the value of the angular velocity $\omega$ for a given $I$ and, by successive evaluations the function $\omega\,(I)$ and thus, as recalled hereafter, the dynamical an kinematic moments of inertia.

## 3 Results

### 3.1 Pairing Strengths and Spreading Around the Fermi Surface

We present here our first results for the first SD band in $^{192}$Hg and $^{194}$Pb nuclei. The governing idea is to compare the Cr. HTDA predictions with those of a Cranking HFB in similar conditions. However, on that purpose, we have to overcross the difficulty to give as input for these different approaches valid couples of pairing strengths $\left(V_0^{protons}, V_0^{neutrons}\right)$, whereas any comparison between correlation energies in HFB and HTDA are meaningless. (The HTDA correlation energy contains clearly pairing correlations but also contributions of different nature.) Having in mind that our present objective is not to fix these constants on the ground of microscopic arguments but to compare the behavior of SD bands on increasing angular momentum when these two approaches are put in similar conditions, we have adopted the following recipe:

i) We have employed in Cranking HFB calculations the values $(V_0^p, V_0^n) = (415, 295)$ MeV which give the convenient values for the moment of inertia of $^{192}$Hg at low spin under our present cutoff condition.

ii) We have considered that a realistic evaluation of the effect of correlations on the wave-function lies in the spreading of the distribution of states around the Fermi energy. This spreading is measured by the sum over the whole space of occupation probabilities $\sum_i u_i v_i$ with usual notation. This quantity being evaluable in both approaches, we have fixed our HTDA strengths ($V_0^p$,$V_0^n$) $= (1550, 1280)$ MeV by the condition to have roughly in both approaches the same spreading $\sum_i u_i v_i$ at no spin for each distribution.

That is illustrated in Figure 1 where the $\sum_i u_i v_i$ functions for proton and for neutron distributions in $^{192}$Hg have been plotted as functions of the angular velocity $\omega$ for Cranking HFB and HTDA calculations. As explained, points at $\omega = 0$ are roughly adjusted to get same results in the two models. On increasing $\omega$, one can see that the HTDA solution remains more correlated and more regular (especially in the proton distribution where one gets a spectacular difference between the two descriptions). Similar behaviors of the spreading function can be observed in Figure 2 for $^{194}$Pb. Calculations for this nucleus have been performed using the same sets of strength parameters.

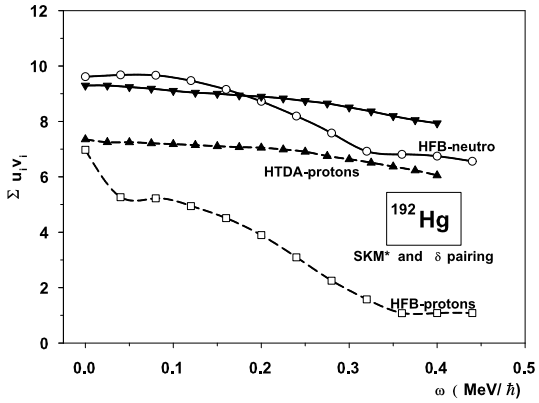


Figure 1. Cranking HFB and HTDA spreading function $\sum u_i\, v_i$ for proton and neutron distributions versus angular velocity $\omega$ in $^{192}$Hg.

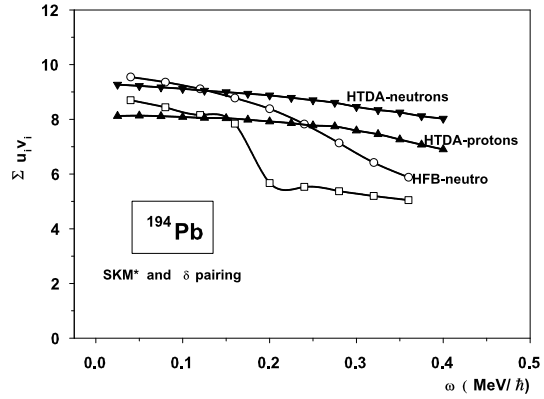


Figure 2. Same as Figure 1 for $^{194}$Pb.

### 3.2 Moments of Inertia in the Yrast SD Bands of $^{192}$Hg and $^{194}$Pb

The theoretical kinetic $J^1$and dynamic $J^2$ moments of inertia have been determined in the usual way (see for instance Refs. [5] or [16]). That means they are completly defined by the calculated function $\left\langle \widehat{J}_x \right\rangle (\omega)$ through the standard formulas:

$$\mathcal{J}^1 = \frac{\left\langle \widehat{J}_x \right\rangle}{\omega} \text{ and } J^2 = \frac{d\left\langle \widehat{J}_x \right\rangle}{d\omega} \tag{13}$$

In practice, the $\mathcal{J}^1$ moment of inertia is directly obtained in each point of calculation, whereas a spline of the function $\left\langle \widehat{J}_x \right\rangle (\omega)$ is needed to get the derivative for $\mathcal{J}^2$.

On another hand, the experimental data for these two quantities is extracted from SD energy sequences available in particular in the sytematic compilation of Ref. [17]. Following the usual definitions employed there, one gets the experimental quantities through the relations:

$$\hbar\omega_{\exp} = \frac{E_\gamma^+(I) + E_\gamma^-(I)}{4} \quad (\text{MeV}) \tag{14}$$

$$\begin{aligned} \mathcal{J}^1_{\exp}(I) &= \frac{4\sqrt{I(I+1)}}{E_\gamma^+(I) + E_\gamma^-(I)} \quad \text{and} \\ \mathcal{J}^2_{\exp}(I) &= \frac{4}{E_\gamma^+(I) - E_\gamma^-(I)} \quad (\hbar^2\text{MeV}^{-1}) \,, \end{aligned} \tag{15}$$

relating angular velocity and moment of inertia at each angular momentum $I$ to the transition energies over and under the considered level observed at the energy $E(I)$ (MeV), namely $E_\gamma^+(I) = E(I+2) - E(I)$ and $E_\gamma^-(I) = E(I) - E(I-2)$.

About theoretical moment of inertia it should be noted that the set of formula Eq. (13) does not involve at all the total energy. That is of some importance and is not related to the precision of calculation and the accuracy of convergence in energy. As matter of fact, the HTDA Hamiltonian is effective in a given space, and the $E^{HTDA}$ energy contains therefore a spurious part which is a priori different for HTDA calculations performed in different configuration spaces (as it is the case for calculations performed in this case at different angular momentum). As a result, that complicates somewhat the evaluation of transition energies between two states belonging to different configuration spaces (see e.g. the discussion of the isomeric state energy in $^{178}$Hf in Ref. [11]) but does not affect at all our present results on $\mathcal{J}^1$ and $\mathcal{J}^2$ moments of inertia.

The $\mathcal{J}^1$ moments of inertia for the first SD band in $^{192}$Hg are displayed in Figure 3 as functions of the angular velocity $\omega$. Results obtained with three cranking approaches are reported and compared with experimental data. One will see on the upper part of the figure the curve labelled "HF", corresponding to a Cranking Hartree-Fock result i.e. a calculation without pairing correlation of any kind. As well known, the initial $\mathcal{J}^1$ value is naturally too high in the absence of superfluid phase, and the variation versus $\omega$ is too slow. This unsurprising result just remind the necessity to take into account pairing correlations to describe the behaviour of SD band moments of inertia in the $A \sim 190$ region. In the middle of the figure, the curve "HFB" corresponding to the Cranking HFB calculation starts quite well but looses too fast the correlations and has a wrong behaviour at high spin as compared with experimental data labelled "Exp". The Cranked HTDA $\mathcal{J}^1$ curve labelled HTDA on the center exhibit a quite convincing regular behaviour in nice agreement with experiment up to high spin.

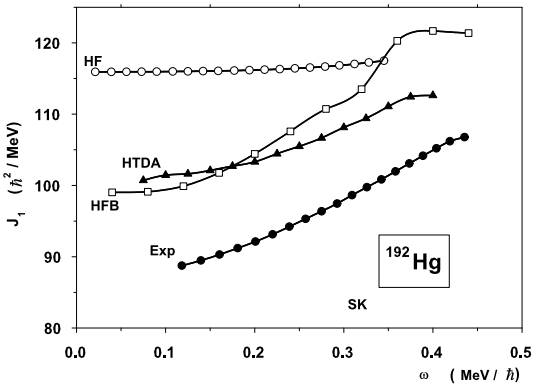


Figure 3. Moment of inertia $\mathcal{J}^1$ in $^{192}$Hg SD band 1 as functions of the angular velocity $\omega$ calculated within cranking approaches HF,HFB and HTDA as labelled and compared with experimental values (Exp).

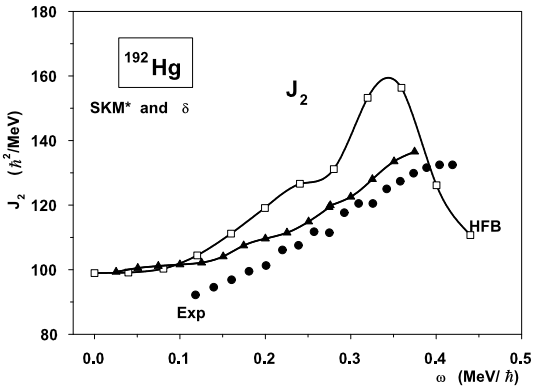


Figure 4. Moment of inertia $\mathcal{J}^2$ in $^{192}$Hg SD band 1 as functions of the angular velocity $\omega$ calculated within two different cranking approaches (HFB and HTDA) and compared with experimental values (Exp).

Cranking HTDA and HFB dynamic moment of inertia $\mathcal{J}^2$ are compared to experimental data in Figure 4 as functions of the angular velocity $\omega$ for the same yrast SD band of $^{192}$Hg. As well known, the function $\mathcal{J}^2$ play the role of a "zoom". Deviations of the Cr. HFB results (due for a part to a lack of correlations at high spin) from experience ("Exp") become drastic, whereas the Cr. HTDA values remain in reasonable agreement for this very "sensitive" function.

Similar calculations have been performed for the $^{194}$Pb SD band 1. Results for moment of inertia $\mathcal{J}^1$ and $\mathcal{J}^2$ are displayed in Figures 5 and 6 respectively. One more time, for this nucleus, the behavior of the $\mathcal{J}^1$ moment of inertia calculated by the present HTDA cranking approach exhibits a regular behavior by far

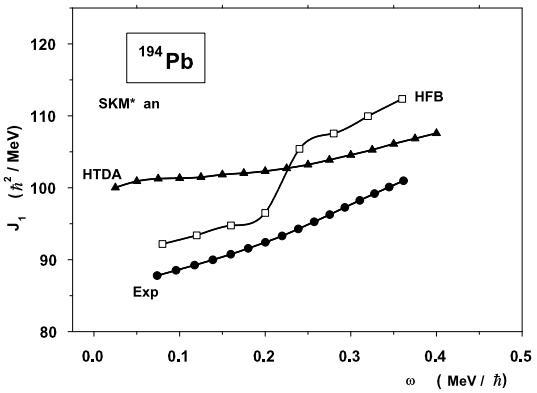


Figure 5. Same as Figure 3 for $^{194}$Pb.

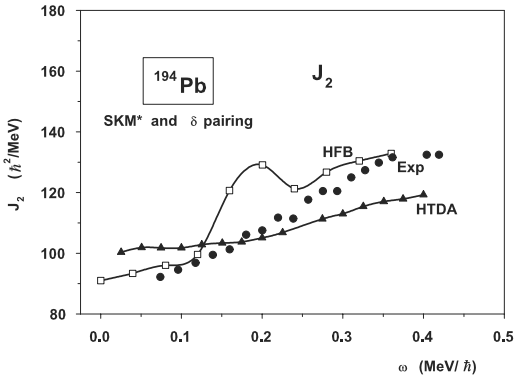


Figure 6. Same as Figure 4 for $^{194}$Pb.

better than those deduced by Cranking HFB. However, a non neglible deviation in slope for the HTDA curve characterise a certain overestimation of correlations at higher spin. Curves for the $\mathcal{J}^2$ moment displayed in Figure 6 confirm and amplify these observations. The Cr. HFB $\mathcal{J}^2$ exhibits an erratic and meaningless behavior, whereas the HTDA curve remains regular but varies somewhat too slowly and and therefore crosses the experimental one in the end.

## 4 Conclusions and Perspectives

This first work within the Cranking HTDA model has shown at least that the general context HTDA is a practicable path to describe nuclear rotational motion. However, as pointed out in the introduction of this paper, we had here to deal without a parametrisation of the pairing interaction built as an effective interaction should be, i.e. available for the whole chart of nucleides and derived within an overall point of view grounded by different evaluations of microscopic quantities. Thus, we did not progress deeply here on the point i) of the introduction, our pairing interaction being an ad hoc one to describe the rotational properties at no spin. It is however noticeable that the spreading in configuration space offers in both contexts Cr. HFB and Cr. HTDA a direct measurement of collective inertial properties of the rotational sequence. That is shown on connecting spreading at low spin displayed in Figures 1 and 2 with first values of moments of inertia to be found in the four other figures. On an other hand (second point of the introduction), in view of present results, Cr. HTDA seems to offer a better understanding of the Coriolis Anti-Pairing mechanism (CAP). Correlations are clearly maintained to higher spin than within a Cr. HFB, and moreover, their evolutions as functions of the angular velocity $\omega$ appears on these exemples mainly correct. The small but observable default in the slope of the moments

of inertia versus spin for $^{194}$Pb indicates however that some progresses are still to be done in the undertanding of the CAP mechanism. A possible limitation introduced by the choice of a pairing interaction of $\delta$ type could be evoked for this point. Finally, the context HTDA, which of course offers in its basic principles a nuclear wave-functions with good number of particles allows to evict the important default of quasiparticle descriptions in weak pairing context. It opens a very large area of investigations offering in particular a theoretical frame in which even, odd-odd and odd-even nuclei can be described in a consistent manner. Various works are thus presently underway in the HTDA context. They are adressed to nuclear structure problems as differents as the evaluation of fission barreers, rotational band in odd nuclei, intrication of RPA correlations and pairing ones. etc... and will offer in coming years, together with present effort to describe the CAP mechanism, an evaluation of the physical content carried by HTDA models.

## Acknowledgment

Part of this work has been funded through the agreement # 12533 between the Bulgarian Academy of Sciences (BAS-Bulgaria) and the Centre National de la Recherche Scientifique (CNRS-France) which are gratefully acknowledged.

## References

[1] J. Libert, M. Girod and J.- P. Delaroche (1999) *Phys. Rev. C* **60** 054301.
[2] H. Laftchiev, D. Samsoen, P. Quentin and I. N. Mikhailov (2003) *Phys. Rev. C* **67** 014301.
[3] H. Flocard, B. Q. Chen, B. Gall *et al.* (1993) *Nucl.Phys. A* **557** 559c.
[4] M. Girod, J. P. Delaroche, J. F. Berger, J. Libert (1994) *Phys. Lett. B* **325** 1.
[5] B. Gall, P. Bonche, J. Dobaczewski *et al.* (1994) *Z. Phys. A* **348** 183.
[6] A. Valor, J. L. Egido, L. M. Robledo (1997) *Phys. Lett. B* **393** 249.
[7] S. Peru (1997) *PHD thesis* Université Paris VII, France.
[8] J. Terasaki, P. -H. Heenen, P. Dobaczewski, H. Flocard (1995) *Nucl. Phys. A* **593** 1.
[9] A. V. Afanasjev, J. Konig, P. Ring (1999) *Phys. Rev. C* **60** 051303.
[10] N. Pillet (2000) *PhD Thesis* Université Bordeaux I, France.
[11] N. Pillet, P. Quentin, J. Libert (2002) *Nucl. Phys. A* **697** 141.
[12] S. J. Krieger, P. Bonche, H. Flocard, P. Quentin (1990) *Nucl. Physics A* **517** 275.
[13] B. N. Parlett and D. N. Scott (1979) *Math. Comp.* **217** 33-145, http://netlib.org/laso/dnlaso.f.
[14] D. Samsoen, P. Quentin, J. Bartel (1999) *Nucl. Phys. A* **652** 34.
[15] A. L. Goodman (1974) *Nucl. Phys. A* **265** 466.
[16] D. Samsoen, H. Laftchiev, P. Quentin and J. Piperova (2001) *Eur. Phys. J. A* **12** 155.
[17] *Table of Superdeformed Nuclear Bands and Fission Isomers* Third Edition July 2002, B. Singh, R. Zywina and R. B. Firestone (2002) *Nucl. Data Sheet* **97** 241.